

CHARACTERIZATION OF FRACTURED GEOTHERMAL RESERVOIR USING SINUSOIDAL FLOW-RATE PRESSURE INTERFERENCE TEST

S. NAKAO & T. ISHIDO

Geological Survey of Japan, AIST, Tsukuba, Japan

SUMMARY – Sinusoidal pressure transient test is one of the periodically changing flow-rate methods to evaluate complicated reservoirs. We have carried out numerical simulation studies to examine optimal sinusoidal flow periods and resulting pressure transient behaviours of an observation well. Three-dimensional porous and double porosity (“MINC”) reservoir models are used. Differences between the pressure response of the porous-medium and the fractured-medium models are discussed. It appears possible to predict whether a reservoir medium between two wells is porous or fractured, when hydraulic diffusivity of several different sinusoidal flow-rate periods can be estimated from a time lag of the pressure interference at an observation well. An example of pressure interference data observed at the geothermal field in Japan is also presented.

1. INTRODUCTION

Pressure interference testing using multiple wells is not only a useful and direct method to collect reservoir information, but also has a possibility to investigate characteristics of naturally fractured reservoir (e.g., Chen et al., 1984). Pressure controlled well tests using periodically changing flow rates are used for pressure interference tests. There are two types of periodically changing flow-rate method; one is the pulse testing method and the other is the sinusoidal method. The pulse testing method developed in petroleum reservoir engineering employs a series of constant flow rate productiodinjection following a shut-in (Johnson et al., 1966). The sinusoidal method, using sine function as the source *pressure or source flow-rate, was developed for the management of nuclear waste disposal (Black et al., 1986). Observable quantities, amplitude attenuation and time lag of the pressure interference at an observation well contain information about reservoir parameters. In particular, a time lag defined independently of pressure response amplitude allows estimation of the degree of heterogeneity between the active well and the observation well. Moreover, it is possible to investigate characteristics of fractures by evaluating the flow-rate period dependence of hydraulic diffusivity calculated from time lags.

Theoretical description of sinusoidal pressure response for pressure-controlled source cases and flow-rate controlled source cases are discussed by Black and Kipp (1981) and Streltsova (1988), respectively. If application to geothermal wells is taken into account, flow-rate controlling procedure will be more suitable because of the simplicity of set-up and the ease of test execution. In the following, the sinusoidal method refers to the one using such a flow-rate controlling procedure.

New Energy and Industrial Technology Development Organization (NEDO) has been developing new techniques for reservoir characterization including a new well testing system (Ide et al., 2000). As part of this project, NEDO has conducted field experiments of pressure controlled well tests such as sinusoidal injection test at the Mori geothermal field in Hokkaido, Japan (Horikoshi et al., 2001). In order to obtain high quality data, development of guidelines for a field test design is very important. To this end, we have conducted a series of numerical calculations to examine optimal sinusoidal flow periods and resulting pressure transient behaviours of injection and observation wells. In these calculations, we used a 3-D reservoir model with a “MINC”-type (Pruess and Narasimhan, 1985) fracture/matrix composite representation. In the following, we will describe the model, and discuss the possibility of characterizing hydrological properties of fractured geothermal reservoirs. The application to the field test data will be also discussed.

2. PRESSURE RESPONSE TO A SINUSOIDAL FLOW RATE

Figure 1 illustrates a pressure interference response at an observation well due to typical sinusoidal flow rate of production/injection for geothermal wells. The pressure amplitude ΔP_p in Figure 1 is given by (Streltsova, 1988):

$$\Delta P_p = \frac{q_0}{2\pi T} \sqrt{\frac{\pi}{2x}} \exp\left(-\frac{x}{\sqrt{2}}\right) \quad (1)$$

where

$$x = r \sqrt{\frac{\omega}{\eta}} \quad (2)$$

In equations 1 and 2, q_0 is the flow rate shown in Figure 1; T is the transmissivity (kh/μ); r is the distance from an active well; ω is the angular frequency ($2\pi/\bar{T}$); \bar{T} is the sinusoidal flow-rate

period; η is the hydraulic diffusivity (T/S); S is the storativity ($\phi C_t h$).

Phase lag ϕ_L and time lag t_L between flow rate and pressure response at the observation well are

$$\phi_L = \frac{x}{\sqrt{2}} + \frac{\pi}{8} = \sqrt{\frac{r^2 \omega}{2\eta}} + \frac{\pi}{8} \quad (3)$$

$$t_L = \frac{\phi_L}{\omega} = \sqrt{\frac{r^2 T}{4\pi\eta}} + \frac{T}{16} \quad (4).$$

If the time lags are successfully observed for several different sinusoidal periods, it is possible to evaluate the sinusoidal period dependence of the hydraulic diffusivity.

3. NUMERICAL SIMULATION USING 3-D RESERVOIR MODEL

3.1 Outline of the model

For our numerical simulation study, we used the **STAR** general-purpose geothermal reservoir simulator (Pritchett, 1995). We used a 3-D reservoir geometry, as illustrated in Figure 2. The reservoir model consists of three parts: a low permeability upper layer A (caprocks); a high permeability middle layer B (reservoir), and a relatively low permeability layer C below the reservoir. A solid circle and an open circle in Figure 2 indicate the injection and the observation wells, respectively. The reservoir is treated either as a simple porous medium or as a "MINC"-type fracture/matrix composite with a fracture spacing of 10, 30 and 100 m.

Constant pressure and temperature (101.3 kPa and 10 °C) are assigned for a ground surface boundary. Temperature increases with depth up to 200 °C. Initial pressure of the injection well and observation well are set to be 13.457 MPa at 1500 m feed-zone depth and 8.333 MPa at 950 m feed-zone depth, respectively. The right side of the reservoir depth is assumed to be a constant pressure boundary. Other boundaries are impermeable and insulated. The kh , storativity and rock properties estimated from well tests and geological analyses of the Mori geothermal field are taken into account in constructing the model. Injection flow rates are changed within 500 kg/min.

3.2 Result and Discussion

Six individual sinusoidal periods of water injection, 6, 12, 24, 48, 72 and 96 hours were used for the numerical calculations to investigate pressure interference response at the observation well. Figure 3 shows calculated pressure histories of the injection and observation wells for the porous-medium and the fractured-medium reservoir model (fracture spacing of 100 m); the

sinusoidal period is 6 hours. For the porous-

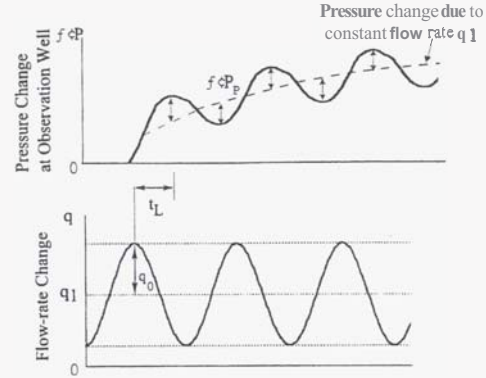


Figure 1. Pressure response to a sinusoidal flow-rate $q(t) = q_1 - q_0 \cos(\omega t)$.

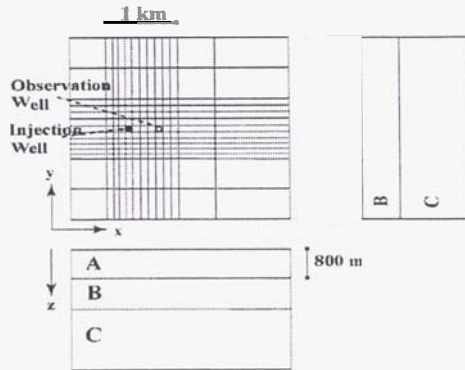


Figure 2. 3-D model geometry used for numerical simulation of sinusoidal tests.

medium case, the sinusoidal pressure response of the observation well cannot be observed. For the fractured-medium case, we can clearly observe the sinusoidal behaviour in the pressure interference. For the fracture-medium case the pressure equilibrium between the fracture zones and rock matrix is not reached, so that only small storativity of fracture zones contributes to the pressure interference response. This is the reason why sinusoidal behaviour is clearly observed in the pressure interference for the fractured-medium case.

The time needed for pressure equilibrium between the fracture zones and rock matrix is given by:

$$\tau_p = \frac{\phi_m C_t \mu \lambda^2}{10 k_m} \quad (5)$$

where λ is average fracture spacing; C_t is a total compressibility; ϕ_m and k_m represent the porosity and permeability of rock matrix, respectively. Before $t = \tau_p$ only small storativity of fracture zones exists, and after τ_p both of fracture zones

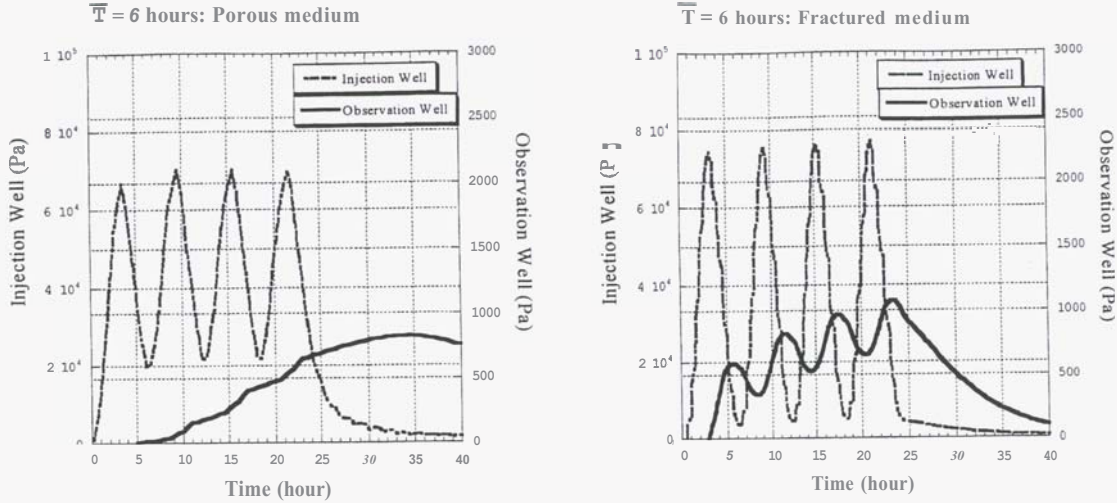


Figure 3. Calculated pressure transients for sinusoidal period of 6 hours. Left column: porous medium model. Right column: fractured medium model with fracture spacing = 100 m ($\lambda^2/k_m = 10^{22}$).

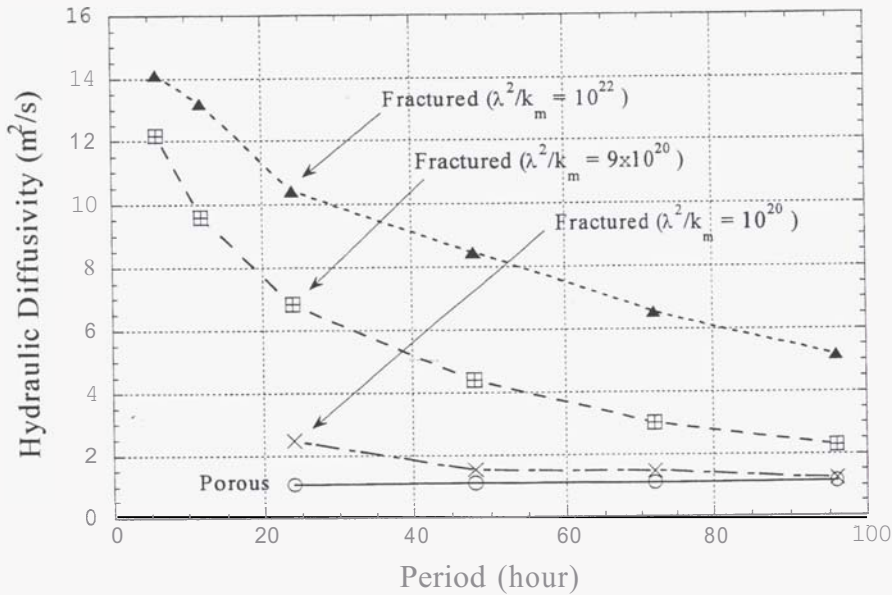


Figure 4. Hydraulic diffusivity estimated from simulated time lag for each sinusoidal period.

and rock matrix storativities contribute to the pressure interference response. The storativity remains constant for the porous-medium case.

Figure 4 shows the estimated hydraulic diffusivity versus sinusoidal period for porous- and fractured-medium cases. After time lags are measured from the numerical simulation results, the hydraulic diffusivity is calculated using Equation 4. The hydraulic diffusivity is independent of the sinusoidal period and has a constant value of $1.1 \text{ m}^2/\text{s}$ for the porous-medium case. By contrast, as the fracture spacing increases (larger λ^2/k_m), the degree of hydraulic diffusivity decline, likewise it increases for the fractured-medium case. When λ^2/k_m is 10^{20} corresponding to a fracture spacing of 10 m, τ_p is estimated as about 6 hours, resulting in the hydraulic diffusivity curve approximately

identical to the porous-medium case. These results suggest that by estimating hydraulic diffusivity using equation 4, it might also be possible to detect whether the reservoir medium is porous or fractured, if we observe the time lags (τ_p) for several sinusoidal periods. When assuming a value for rock matrix permeability, average fracture spacing can also be estimated.

4. ANALYSIS OF THE FIELD TEST DATA

Pressure interference data obtained by NEDO at the Mori geothermal field is discussed below. Figure 5 shows injection flow rates at the injection well and the observed pressure interference response at the observation well. The distance between the two feed zones is approximately 720 m. Two types of injection, a nearly constant

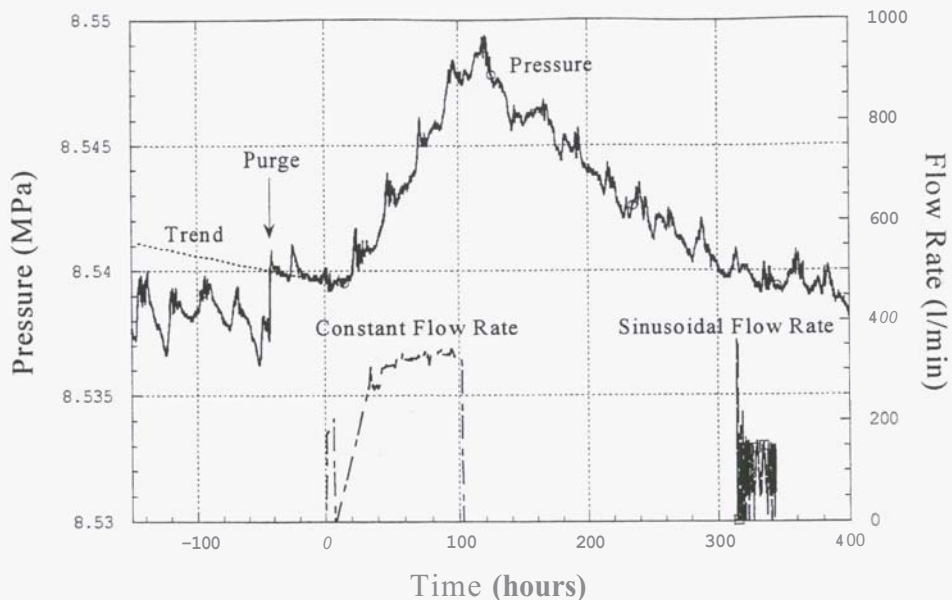


Figure 5. Actual injection flow-rate history at the injection well and pressure interference response at the observation well in the Mori geothermal field.

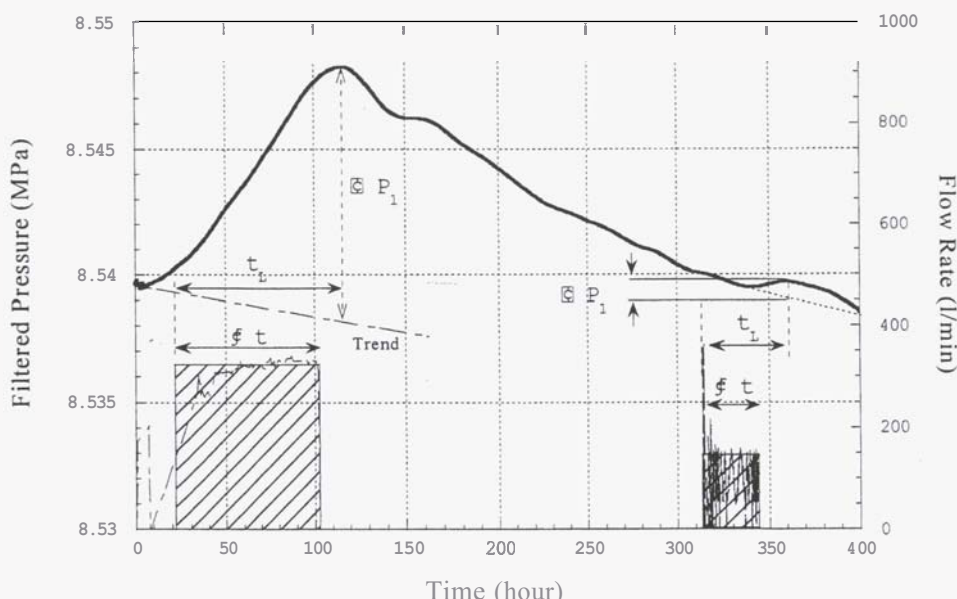


Figure 6. Pressure interference data with background noise removed by low-pass filter. A series of sinusoidal injection is treated as a constant flow-rate pulse.

4-day injection and a series of sinusoidal injections within 10, 30, 100, and 300 minutes periods, were conducted. Background noise of short wavelength is notably contained in the pressure interference signal. The noise obscures the sinusoidal behaviour of the pressure interference signals, which correspond to the sinusoidal injection. Thus, it was not possible to detect whether the medium between the two wells is of a porous- or fractured-medium type.

The pressure interference signals corresponding to the constant flow rate are large enough and suitable for analysis. We carried out inversion analyses of this interference data based upon a line-source model. Calculated kh and storativity

are $7.40 \times 10^{-12} \text{ m}^3$ and $1.23 \times 10^{-7} \text{ m/Pa}$, respectively. An inversion analysis based upon a "double porosity" model was also performed in order to investigate the fractures. There is, however, only a little difference in the matching errors between the result of the porous model and the double porosity model, so that it is difficult to evaluate characteristics of the medium from the pressure interference data due to the constant flow rate.

Figure 6 shows the pressure interference data with background noise removed using a low-pass filter.

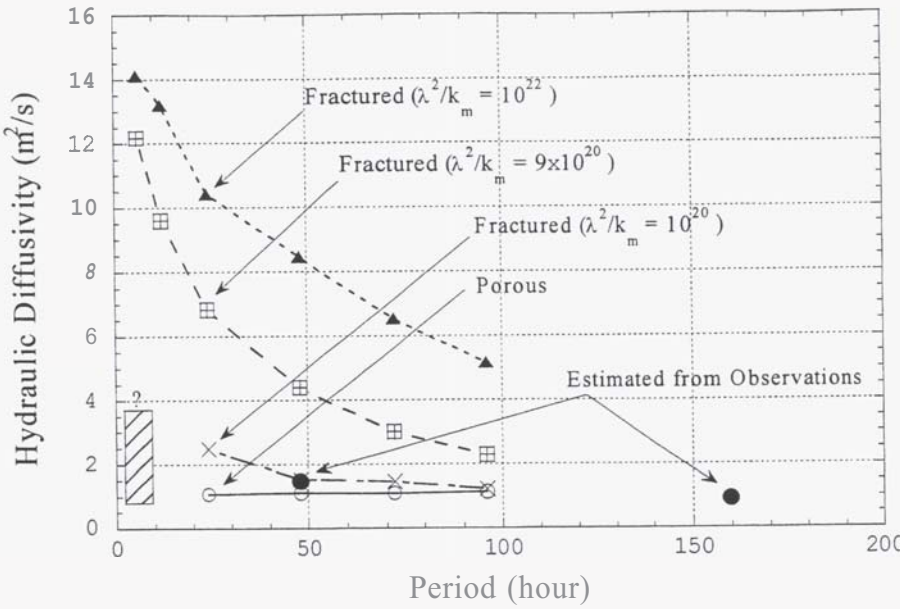


Figure 7. Dependence of hydraulic diffusivity on sinusoidal periods between two wells at the Mori geothermal field.

Although it is impossible to extract the individual pressure interference signal corresponding to each sinusoidal flow rate, the pressure interference corresponding to a series of sinusoidal injection (for a whole day) can be observable by filter processing of 20-hour corner frequency. Hence, as shown in Figure 6, we will assume two injection events (two pulse testings) as a four-day constant flow-rate injection and a one-day constant flow-rate injection, and try to calculate hydraulic diffusivities from time lags corresponding to two different pulse times.

For pulse testing procedure the relationship among hydraulic diffusivity, pulse time At (equivalent to the half of a sinusoidal period), and time lag t_L (Fig. 6) at which the pressure response has a maximum value is expressed by (Streltsova, 1988):

$$\frac{r^2}{4\eta\Delta t} = -\frac{t_L}{\Delta t} \left(\frac{t_L}{\Delta t} - 1 \right) \ln \left(1 - \frac{\Delta t}{t_L} \right) \quad (6)$$

For the four-day constant (pulse) injection, it can be determined that the pulse time is $At = 80$ hours and the time lag is $t_L = 100$ hours. Therefore, the hydraulic diffusivity $\eta = 0.89 \text{ m}^2/\text{s}$ is obtained from Equation 6, where $r = 720 \text{ m}$. Similarly, for the one-day pulse injection the hydraulic diffusivity $\eta = 1.47 \text{ m}^2/\text{s}$ is obtained from the calculation using $At = 24$ hours and $t_L = 40$ hours.

The pulse times $At = 80$ hours and 24 hours are equivalent to the sinusoidal periods of 160 and 48

hours, respectively. These hydraulic diffusivity values are plotted on the sinusoidal period versus hydraulic diffusivity curve derived from the numerical simulation of the 3-D reservoir model (Fig. 7). Although the actual sinusoidal periods used were 10 min, 30 min, 100 min and 300 min, hydraulic diffusivities are not estimated due to the noise during these periods, shown as a hatched area in Figure 7. In the numerical calculation of the 3-D model, it is also difficult to read time lags in the cases of 6-hour and 12-hour sinusoidal periods for the porous model (see Fig. 3) and fractured model with $\lambda^2/k_m = 10^{20}$.

From the result shown in Figure 7, it can be seen firstly that the hydraulic diffusivities detected from the observed data are consistent with those from numerical simulations of the 3-D model; this suggests the validity of the 3-D numerical model and that the analytical line-source solution gives a good approximation to the 3-D numerical model in this case. Secondly, as the pulse time increases, the hydraulic diffusivity calculated from the observed data decreases as well as those obtained from numerical simulations for the fractured model. Since the hydraulic diffusivity is close to the result of numerical simulation of $\lambda^2/k_m = 10^{20}$, average fracture spacing λ can be estimated as 10 m, 30 m and 100 m, assuming rock matrix permeability k_m of 10^{-18} m^2 , 10^{-17} m^2 and 10^{-16} m^2 , respectively.

5. CONCLUSIONS

We have conducted numerical simulation studies on the pressure responses of sinusoidal injection flow-rate tests to examine the resulting pressure interference response of the observation well. The result is described below.

The sinusoidal behaviour can be discerned more clearly in the pressure interference for the fractured-medium model than that for the porous-medium model. This suggests that during the estimation hydraulic diffusivity, it might also be possible to detect whether the reservoir medium is porous or fractured, if we observe the time lags (t_L) for several sinusoidal periods.

The pressure interference data observed at the Mori geothermal field was analysed as a pulse testing method. The medium between two wells appears to be of the fractured-type, because estimated hydraulic diffusivity are similar to the numerical results for the fractured-medium case.

6. ACKNOWLEDGEMENTS

The authors would like to thank the New Energy and Industrial Technology Development Organization for permission to use the well test data.

7. REFERENCES

Black, J. H. and Kipp, K. L. Jr. (1981). Determination of hydrogeological parameters using sinusoidal pressure tests: A theoretical appraisal. *Water Res. Res.*, 17, 686-692.

Black, J. H., Barker, J. A. and Noy, D. J. (1986). *Crosshole investigations- The method, theory and analysis of crosshole sinusoidal pressure tests in fissured rock*. STRIPA Project 86-03, Swedish Nuclear Fuel and Waste Management co.

Chen, C. C., Yeh, N., Raghavan, R. and Reynolds, A.C. (1984). Pressure response at observation wells in fractured reservoirs. *Soc. Pet. Eng. J.*, 24, 628-638.

Horikoshi, T., Yamazawa, S., Ide, T. and Toshia, T. (2001). NEDO's project on development of technology for reservoir mass and heat flow characterization. Project outline and techniques to improve the reservoir model, *GRC Transactions*, 25, 641-644.

Ide, T., Yamazawa, S. and Toshia, T. (2000). The development of a computerized pressure transient test system (Part 1). *Proc. 25th Workshop on Geothermal Res. Eng.*, Stanford University.

Johnson, C. R., Greenkorn, R. A. and Woods, E.G. (1966). Pulse testing: A new method for describing reservoir flow properties between wells. *J. Pet. Tech.*, Dec. 1599-1604.

Pritchett, J. W. (1995). *STAR User's Manual*. Report SSS-TR-92-13366, S-Cubed.

Pruess, K. and Narasimhan, T.N. (1985). A Practical Method for Modeling Fluid and Heat Flow in Fractured Porous Media. *Soc. Pet. Eng. J.*, February, 14-26.

Streltsova, T. D. (1988). *Well Testing in Heterogeneous Formations*. John Wiley & Sons, New York.